Nordic Seas Hydrography in the Context of Arctic and North Atlantic Ocean Dynamics

J. S. KENIGSON[a] AND M.-L. TIMMERMANS[a]

[a] *Department of Earth and Planetary Sciences, Yale University, New Haven, Connecticut*

(Manuscript received 31 March 2020, in final form 19 October 2020)

ABSTRACT: The hydrography of the Nordic seas, a critical site for deep convective mixing, is controlled by various processes. On one hand, Arctic Ocean exports are thought to freshen the North Atlantic Ocean and the Nordic seas, as in the Great Salinity Anomalies (GSAs) of the 1970s–1990s. On the other hand, the salinity of the Nordic seas covaries with that of the Atlantic inflow across the Greenland–Scotland Ridge, leaving an uncertain role for Arctic Ocean exports. In this study, multidecadal time series (1950–2018) of the Nordic seas hydrography, Subarctic Front (SAF) in the North Atlantic Ocean [separating the water masses of the relatively cool, fresh Subpolar Gyre (SPG) from the warm, saline Subtropical Gyre (STG)], and atmospheric forcing are examined and suggest a unified view. The Nordic seas freshwater content is shown to covary on decadal time scales with the position of the SAF. When the SPG is strong, the SAF shifts eastward of its mean position, increasing the contribution of subpolar relative to subtropical source water to the Atlantic inflow, and vice versa. This suggests that Arctic Ocean fluxes primarily influence the hydrography of the Nordic seas via indirect means (i.e., by freshening the SPG). Case studies of two years with anomalous NAO conditions illustrate how North Atlantic Ocean dynamics relate to the position of the SAF (as indicated by hydrographic properties and stratification changes in the upper water column), and therefore to the properties of the Atlantic inflow and Nordic seas.

KEYWORDS: Ocean; Arctic; North Atlantic Ocean; Atmosphere-ocean interaction

1. Introduction

a. The Nordic seas in the climate system

The Nordic seas (i.e., Greenland, Iceland, and Norwegian Seas; Fig. 1), a transitional region between the Arctic Ocean north of Fram Strait and the North Atlantic Ocean, are a site of key climate processes. Deep convective mixing, a driver of the thermohaline circulation, takes place in the Nordic seas where wintertime air–sea heat fluxes destabilize the stratification and produce deep mixed layers (Nilsen and Falck 2006); further, upper-ocean salinity anomalies are observed to precondition the stratification for deep convection (e.g., Latarius and Quadfasel 2016; Lauvset et al. 2018). Although deep convective mixing also occurs in the Labrador Sea and subpolar North Atlantic Ocean, water mass transformation in the Nordic seas is the dominant contributor to the overturning circulation (Lozier et al. 2019; Chafik and Rossby 2019). Therefore, the processes that determine the Nordic seas hydrographic variability are of considerable scientific interest.

At Fram Strait, the East Greenland Current carries ~4–11 Sv ($1\ \text{Sv} \equiv 10^6\ \text{m}^3\ \text{s}^{-1}$) of relatively cold, fresh Polar Water south to the Nordic seas (de Steur et al. 2009). In addition, about 8 Sv of warm, saline Atlantic Water (the Atlantic inflow) flows northward into the Nordic seas across the Greenland–Scotland Ridge in multiple current systems (Hansen and Østerhus 2000). In one view, Nordic seas hydrographic variability is explained primarily by Arctic exports, which are governed by the Arctic Ocean circulation, particularly the Beaufort Gyre (Dukhovskoy et al. 2004, 2006a,b; Proshutinsky et al. 2015). In another view, the Atlantic inflow determines the Nordic seas salinity variability, leaving a peripheral role for Arctic Ocean dynamics (Glessmer et al. 2014). The complete picture is likely more complicated; for example, Reverdin (2014) points out that Arctic freshwater exports may ultimately feed the Atlantic inflow. Here we propose a conceptual model, consistent with observations, in which Arctic exports and North Atlantic Ocean dynamics interact to explain the Nordic seas hydrographic variability.

b. Arctic Ocean exports freshen the subpolar gyre

Freshwater pulses from the Arctic have been implicated in the "Great Salinity Anomalies" (GSAs) of the 1970s–1990s; the propagation pathways inferred from these events attest to an advective linkage between the Arctic Ocean and the Nordic seas via the Atlantic inflow (Dickson et al. 1988; Belkin et al. 1998; Belkin 2004). The first reported GSA likely originated in the late 1960s as a ~2000 km^3 sea ice/freshwater pulse at Fram Strait, which was subsequently advected into the subpolar gyre (SPG); it then propagated cyclonically, reentered the Nordic seas via the Atlantic inflow, and recirculated into the Greenland Sea in 1981–82 (Dickson et al. 1988). While subsequent GSAs have been attributed to Davis Strait exports and/or processes local to the Labrador Sea, the anomalies have been suggested to have propagated along similar advective pathways.

Arctic ocean freshwater exports are also thought to be responsible for decadal to multidecadal freshening trends in the subarctic seas. The SPG and Nordic seas accumulated ~10 000 km^3 of freshwater between the late 1960s to early 1970s and ~19 000 km^3 between the mid-1960s and mid-1990s (Curry and Mauritzen 2005); these trends can largely be accounted for by Arctic freshwater anomaly budgets, including sea ice melt and precipitation minus evaporation ($P - E$;

Supplemental information related to this paper is available at the Journals Online website: https://doi.org/10.1175/JPO-D-20-0071.s1.

Corresponding author: Jessica Sarah Kenigson, jessica.kenigson@colorado.edu

DOI: 10.1175/JPO-D-20-0071.1

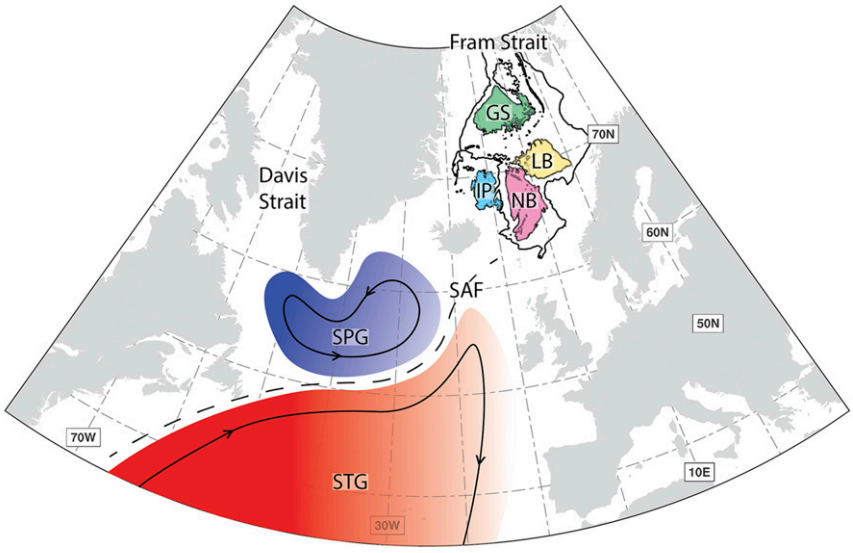

FIG. 1. Bold black contours in the Nordic seas represent the 3000- and 1600-m isobaths, which define the deep basins of Greenland Sea (GS; green), Lofoten Basin (LB; yellow), Norwegian Basin (NB; pink), and Icelandic Plateau (IP; cyan). The blue (SPG) and red (STG) areas represent schematic illustrations of the North Atlantic Ocean gyres and the extent of the associated water masses. The SAF (black dashed line) is the broad boundary between these regions.

Peterson et al. 2006). Models and observations have also linked a freshening of the SPG and Nordic seas in the early 1990s to an enhancement of Arctic Ocean outflows (Karcher et al. 2005). Using hydrographic data, Florindo-López et al. (2020) have demonstrated a correlation between the Arctic freshwater export at the Labrador Shelf and the freshwater content of the subpolar North Atlantic Ocean from 1950 to near present.

Subpolar freshening events have been linked to changes in the Arctic Ocean's wind-driven circulation. Anticyclonic winds associated with the Beaufort high converge available surface freshwater in the Beaufort Gyre system centered over the Canada Basin (Proshutinsky et al. 2002, 2009, 2019b). The strengthening (weakening) of the atmospheric forcing leads the Beaufort Gyre to accumulate (release) freshwater on interannual to decadal time scales, and GSA events broadly coincide with Beaufort Gyre relaxations (e.g., Proshutinsky et al. 2015). The persistent anticyclonic forcing during 1997–2018 was consistent with an observed liquid freshwater increase in the Beaufort Gyre of ~6400 km^3 during 2003–18 (Proshutinsky et al. 2019b). It is unclear whether this freshwater retention has translated to a salinification of the Nordic seas.

c. *North Atlantic Ocean dynamics and the Atlantic inflow*

The Atlantic inflow is comprised of both subpolar gyre and subtropical gyre (STG) source waters (e.g., Hátún et al. 2005). The North Atlantic Current, an extension of the Gulf Stream, transports STG waters to the northeast North Atlantic Ocean, where they undergo mixing with SPG waters and modification before continuing northward into the Nordic seas. Hátún et al. (2005) found that the Atlantic inflow salinity covaries with a "gyre index" representing the strength and spatial extent of the SPG; when the gyre index is positive, the SPG circulation is anomalously strong, the Subarctic Front (SAF; the boundary between subpolar and subtropical water masses) shifts eastward, the Atlantic inflow comprises an increased ratio of SPG to STG source water, and vice versa (Hátún et al. 2005).

The properties of the subtropical and subpolar water masses, and the position of the SAF, are influenced by the atmospheric forcing characterized by the North Atlantic Oscillation (NAO) and East Atlantic Pattern (EAP). The NAO represents the sea level pressure gradient between the Icelandic low and Azores high (Hurrell 1995); changes in the NAO index correspond to wind stress and air–sea heat flux anomalies in the SPG, as well as ocean circulation changes that lead to SAF shifts (Visbeck et al. 2003; Bersch et al. 2007; Sarafanov et al. 2008; Lozier and Stewart 2008). Sarafanov (2009) showed a correlation between the NAO index and the salinity of the Iceland–Scotland Overflow Water (formed in the Nordic seas), inferring that the relative contributions of SPG and STG parent waters to the Nordic seas could vary with the SAF position.

The EAP, the second mode of North Atlantic sea level pressure variability, is associated with wind stress curl anomalies that induce Ekman divergence in the SPG and convergence in the STG, modulating the circulation of both gyres in phase (Häkkinen et al. 2011). By performing tracer advection experiments, Häkkinen et al. (2011) have shown that the weakening of both gyres coincides with a contraction of the SPG and an expansion of the STG, opening a pathway for STG water to penetrate the northeast North Atlantic Ocean (see Hátún et al. 2005). Thus, the positive phase of the EAP is associated with a strengthened (and expanded) SPG and a fresher Atlantic inflow (and vice versa).

d. Nordic seas hydrographic variability: A unified perspective

The Nordic seas hydrography has undergone considerable change during recent decades in which Arctic Ocean outflows and the Beaufort Gyre's freshwater storage have been relatively well observed. The Greenland Sea has warmed and salinified during ~2000–16, leading to an increase in wintertime mixed layer depths (Lauvset et al. 2018), while the Norwegian Sea (containing the Norwegian and Lofoten basins) has freshened during ~2011–18 (Mork et al. 2019). These events have been linked to changes in the Atlantic inflow properties, the cause of which remains unclear. For instance, SAF displacements as indicated by sea surface height contours have been found to be small and unable to explain the water properties of the eastern North Atlantic Ocean (Foukal and Lozier 2017), although this has been questioned (Hátún and Chafik 2018). Furthermore, the relationship between the Atlantic inflow and the recent Beaufort Gyre freshening (with implications to freshwater fluxes from the Arctic) remains unexplored.

In this study, we examine hydrographic variability in the Nordic seas over almost seven decades (starting in 1950) in the context of both Arctic and North Atlantic influences and show that the influence of freshwater that originates in the Arctic necessarily depends on SPG and STG dynamics, including SAF shifts. We first analyze observations to characterize the hydrographic variability of the Nordic seas' deep basins during 1950–2018, extending the 2001–16 reconstruction that Latarius and Quadfasel (2016) derived from Argo data. Next, we compare observations of the Atlantic inflow and Nordic seas water properties to the state of the Arctic Ocean circulation, including the Beaufort Gyre freshwater content and Arctic–subarctic freshwater fluxes. We show how the SAF position relates to the spatial extent of SPG and STG waters in the North Atlantic Ocean, as indicated by stratification changes, and to the Nordic seas freshwater content. Finally, we discuss how NAO-linked ocean circulation changes relate to the SAF and the recent freshening of the northeast North Atlantic Ocean, which likely explain the recent freshening of the Norwegian Sea.

2. Data and methods

a. Data sources

We use observations from the Met Office Hadley Centre EN4.2.1 data (EN4), which consists of two products: 1) a collection of quality-controlled, resampled hydrographic profiles from the World Ocean Database, ARGO, ASBO, and GTSPP; and 2) a 1° × 1° gridded objective analysis, constructed from the profiles, on 42 nonuniformly spaced depth levels between the surface and ~5300 m (Good et al. 2013). The EN4 data have been used extensively in studies of the North Atlantic Ocean hydrography (e.g., Robson et al. 2016; Grist et al. 2016; Foukal and Lozier 2017; Josey et al. 2018; Holliday et al. 2020).

To quantify the SPG circulation variability, we use the SSALTO/DUACS absolute dynamic topography product derived from multisatellite altimetry, which has daily temporal resolution from 1993 to present and 0.25° × 0.25° spatial resolution (Taburet et al. 2019). To investigate the atmospheric state, we use the annual mean, station-based NAO index (Hurrell 1995) and the annual mean EAP index (Barnston and Livezey 1987). Finally, we use monthly means of the NCEP/NCAR Reanalysis I wind stress curl (from 1948 to present) (Kalnay et al. 1996).

b. Reconstruction of the Nordic seas hydrographic variability

Time series (1950–2018) of potential temperature and salinity are constructed in four regions of the Nordic seas: the Greenland Sea (GS), Icelandic Plateau (IP), Norwegian Basin (NB), and Lofoten Basin (LB). We use similar deep-basin definitions as Latarius and Quadfasel (2016), where the 3000-m bathymetric contour defines the GS, NB and LB and the 1600-m contour defines the IP (bathymetry is from the ETOPO 1-arc-min analysis; Amante and Eakins 2009). As the EN4 objective analysis relaxes to a long-term climatology in the absence of observations (Good et al. 2013), potentially introducing artifacts and aliasing hydrographic variability during decades of sparse data coverage, we use the profile data for this purpose. If a profile contains more than 10 valid observations in the vertical, it is linearly remapped onto a common grid with 0.25° × 0.25° horizontal resolution and nonuniform vertical resolution, then averaged over each month and basin. Next, we form anomalies as the difference between the long-term mean and the monthly climatology.

Finally, we examine water-mass types by partitioning the buoyancy frequency N^2 into contributions from vertical temperature gradients ($N^2_T = g\alpha d\Theta/dz$) and salinity gradients ($N^2_S = -g\beta dS/dz$), where g is gravity, Θ is Conservative Temperature, S_A is Absolute Salinity (hereafter S), α is the coefficient of thermal expansion, and β is the coefficient of haline contraction (see McDougall and Barker 2011). This partitioning allows us to delineate water columns that are predominantly stratified by salinity (a characteristic of polar, β oceans) and those that are predominantly stratified by temperature (a characteristic of α oceans) in this region of the North Atlantic and Nordic seas at the confluence of α and β water masses (Carmack 2007; Stewart and Haine 2016).

Using the EN4 gridded objective analysis, we construct time series of the annual mean liquid freshwater content (FWC) in the Nordic seas during 1950–2018. Specifically, the FWC of the water column between the surface and a depth H is defined as

$$\mathrm{FWC} = \int_H^0 \frac{S_{\mathrm{ref}} - S}{S_{\mathrm{ref}}} dz, \tag{1}$$

where S_{ref} is a reference salinity taken to be 34.8 for comparison with prior studies (Aagaard and Carmack 1989; de Steur et al. 2009; Haine et al. 2015; de Steur et al. 2017, 2018; Proshutinsky et al. 2019a,b). While choices of S_{ref} and H have varied among studies (Haine et al. 2015), H is typically taken to be the depth of the isohaline S_{ref}. However, unless salinity dominates the density stratification, this level may not be well defined, necessitating a different choice of H. Since deep convective mixing redistributes freshwater vertically, H should

exceed the maximum mixed layer depth. Here, we take H = 2000 m, and where the bathymetry is shallower than 2000 m, we take H to be the approximate bottom depth. Schauer and Losch (2019) have recently questioned the physical relevance of FWC, given that there is no canonical choice of S_{ref}. Nevertheless, our study is more focused on FWC changes (i.e., anomalies) rather than absolute inventories, which are relatively insensitive to the choice of S_{ref}. To estimate total FWC, we approximate the Nordic seas by a box of area $\sim 2.2 \times 10^6\,\text{km}^2$, bounded to the south by the 63.5°N parallel, the north by the 79.5°N parallel, the west by the 22.5°W meridian, and the east by the 19.5°E meridian.

c. *The subarctic front and the gyre index*

Using the annual mean EN4 objective analysis, we construct two different indices of the SAF position: 1) the zonal extent of the 10°C isotherm at 10-m depth (Roden 1991; Belkin and Levitus 1996; Carmack 2007) and 2) the zonal extent of the 35.0 isohaline at 250-m depth (Sarafanov et al. 2008; Sarafanov 2009). The gyre index, a proxy for the SPG circulation, has been defined as the first principal component of SSH variability, although the spatial domain in the North Atlantic Ocean has varied among studies (Häkkinen and Rhines 2004; Hátún et al. 2005; Berx and Payne 2017; Foukal and Lozier 2017). Since an EOF-based gyre index is sensitive to the SSH product's spatial resolution and temporal coverage (Hátún and Chafik 2018), and may be influenced by the basin-scale sea level rise signal (Foukal and Lozier 2017), we use a more direct metric: the area-mean, detrended SSH in the SPG. Specifically, we construct this index from the SSALTO/DUACS data over a region approximately bounded by the 50° and 65°N parallels and the 60° and 25°W meridians.

3. Arctic–North Atlantic Ocean connections

a. *Nordic seas hydrographic properties: Decadal variability*

The mean hydrographic properties in the Nordic seas reflect 1) an Arctic domain (i.e., the Greenland Sea and Icelandic Plateau), characterized by relatively freshwater overlying saltier water (i.e., characterizing a β ocean), and 2) an Atlantic domain (i.e., the Lofoten Basin and Norwegian Basin), characterized by relatively warm water overlying colder water, an α ocean (Fig. 2); salinity and temperature anomalies relative to the 1950–2018 mean are shown in Fig. 3. In the Arctic domain, the salinity stratification is strongly stable everywhere ($N_S^2 > 0$), with an unstable temperature stratification ($N_T^2 < 0$) notable in the upper water column and N_T^2 weakly positive elsewhere (Figs. 4a,b,e,f). In the Atlantic domain, the temperature stratification is strongly stable everywhere ($N_T^2 > 0$), with salinity stratification generally unstable ($N_S^2 < 0$; Figs. 4c,d,g,h).

Warm saline and cool fresh conditions covary within and among the deep basins on decadal time scales (Fig. 3). Salty conditions have generally coincided with warm conditions, except before ~1960, and the mid-to-upper ocean was anomalously saline during the 1950s–1970s and from around the mid-2000s to near present. During the 1980s–1990s, relatively fresh conditions prevailed alongside a cooler water column. These overall variations are most easily seen in the annual mean Nordic seas FWC (Fig. 5f). Notably, the past-decade warming and salinification of the Arctic domain (Figs. 3a,b,e,f) coincides with a weakening of the salinity stratification (i.e., erosion of the halocline; Figs. 4a,b) that is consistent with a possible *Atlantification* trend (i.e., the incursion of North Atlantic water-mass types north into the Nordic seas and Arctic Ocean; see, e.g., Årthun et al. 2012). In the most recent few years, the salty conditions that have prevailed in the Nordic seas since the early 2000s are giving way to fresher conditions [see Mork et al. (2019), who suggest this may have originated in the Atlantic inflow], while the Arctic domain has remained relatively saline (Figs. 3a–d). Overall, the Nordic seas FWC increased by $\sim 900\,\text{km}^3$ between 2016 and 2018.

b. *Beaufort Gyre freshwater budget and the salinification of the Nordic seas*

We may examine the relationship between Arctic Ocean freshwater fluxes and the Nordic seas in recent decades for which there are sufficient observations. While the Nordic seas were anomalously salty from the early 2000s to the late 2010s, the Beaufort Gyre accumulated freshwater (Giles et al. 2012; Proshutinsky et al. 2015, 2019a; Zhong et al. 2019; Proshutinsky et al. 2019b) at a rate of around 400–550 $\text{km}^3\,\text{yr}^{-1}$ during 2003–18 (Proshutinsky et al. 2019b). Therefore, if the freshwater retention was translated to a reduction in freshwater export to the North Atlantic Ocean, its magnitude would be sufficient to explain the salinification trend in the Nordic seas during the mid-1990s to 2010s: Nordic seas FWC declined from a relative maximum around 1996–2011 at a rate of $\sim 200\,\text{km}^3\,\text{yr}^{-1}$ and remained approximately constant through 2015 (Fig. 5f). This is a purely budgetary comparison; North Atlantic Ocean dynamics, including the SAF position, could largely confine the Arctic freshwater fluxes to the SPG (section 3c). Furthermore, Arctic Ocean FWC is not in a long-term equilibrium and an increase in hydrological inputs would give rise to an increase in Beaufort Gyre freshwater without reducing the Arctic freshwater flux.

About half of Arctic freshwater export is via Fram Strait and the other half is via Davis Strait (Haine et al. 2015). Each of these may influence Nordic seas hydrography. Freshwater export in the East Greenland Current (monitored at Fram Strait since 1997) has been estimated to be around $1060 \pm 394\,\text{km}^3\,\text{yr}^{-1}$ (de Steur et al. 2009, 2017, 2018). While seasonal to interannual variability has been noted, there is no significant long-term trend in Fram Strait freshwater fluxes from 1997 to near present (de Steur et al. 2009, 2018). Further, there was no measurable trend in Davis Strait freshwater flux during 2004–10, when the outflow was monitored by a mooring array (Curry et al. 2014). It, therefore, would seem unlikely that Arctic Ocean processes were responsible for the decadal salinification trend in the Nordic seas from the mid-1990s to 2010s.

c. *Subarctic frontal displacements and the hydrography of the Nordic seas*

The SAF is a broad transitional zone between the α ocean to the south, and the predominantly salinity stratified β ocean to the north (Carmack 2007; Stewart and Haine 2016; Figs. 6a–d). Historically, its location has been approximated by the outcropping of the 10°C isotherm (Figs. 6a–d), particularly in

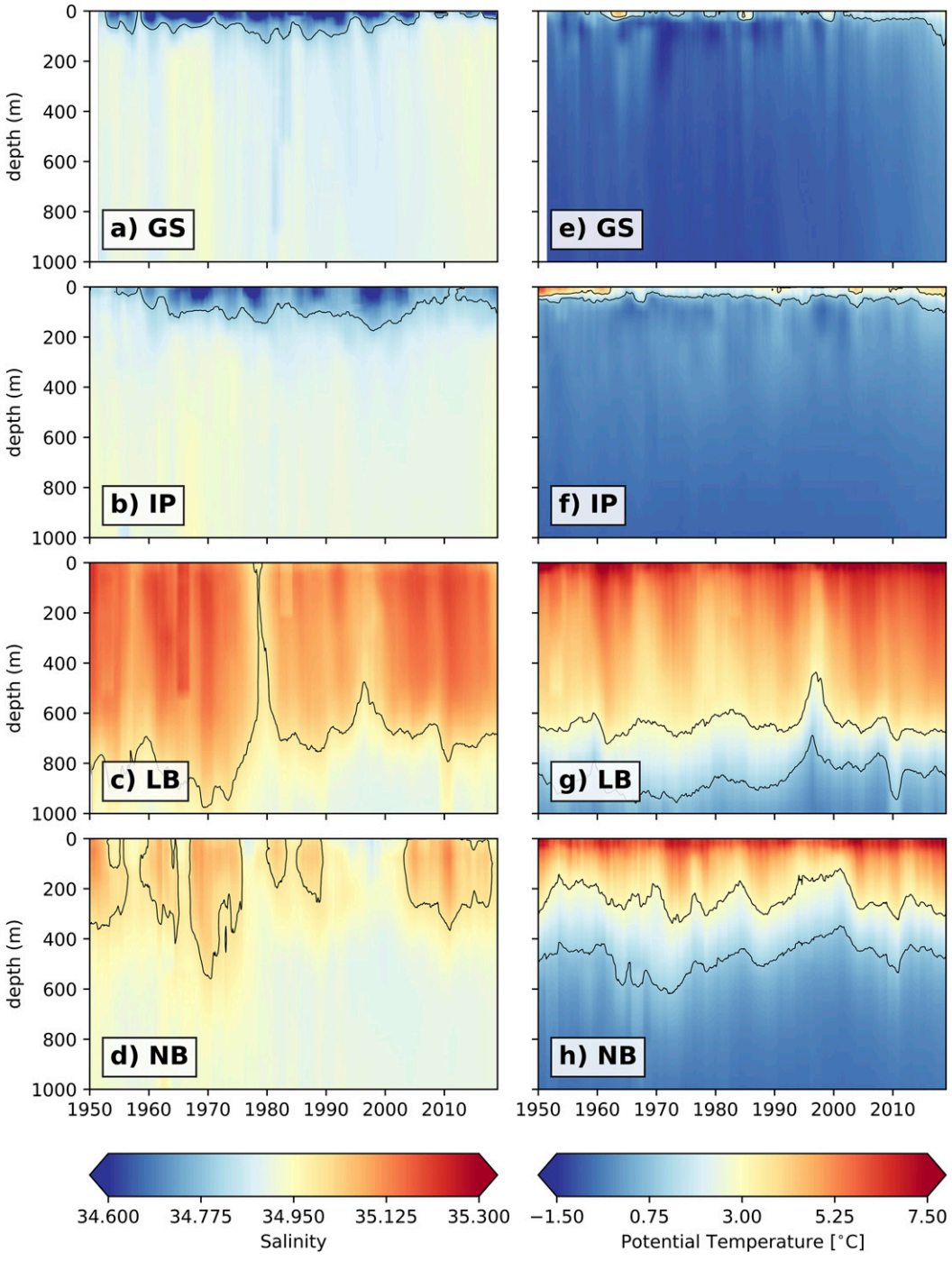

FIG. 2. Time series of (a)–(d) salinity and (e)–(h) potential temperature derived from the EN4 quality-controlled profiles averaged in the deep basins [Greenland Sea (GS), Lofoten Basin (LB), Norwegian Basin (NB), and Icelandic Plateau (IP)] of the Nordic seas for 1950–2018. Data are interpolated monthly means, smoothed with a 25-month centered moving average. Contours indicate the 34.8 and 35 isohalines in (a)–(d) and the 1° and 3°C isotherms in (e)–(h). See Fig. S1 in the online supplemental material that shows the data without interpolation and smoothing.

winter (Roden 1991; Belkin and Levitus 1996). The SAF is also associated with the isoline of zero wind stress curl, separating the cyclonic SPG from the anticyclonic STG (Carmack 2007). The location of the 10°C isotherm closely coincides with the zero contour of N_S^2 at ~210 m, particularly in the western North Atlantic (Figs. 6c,d). The position of the SAF regulates the water mass types that enter the Nordic seas from the North Atlantic.

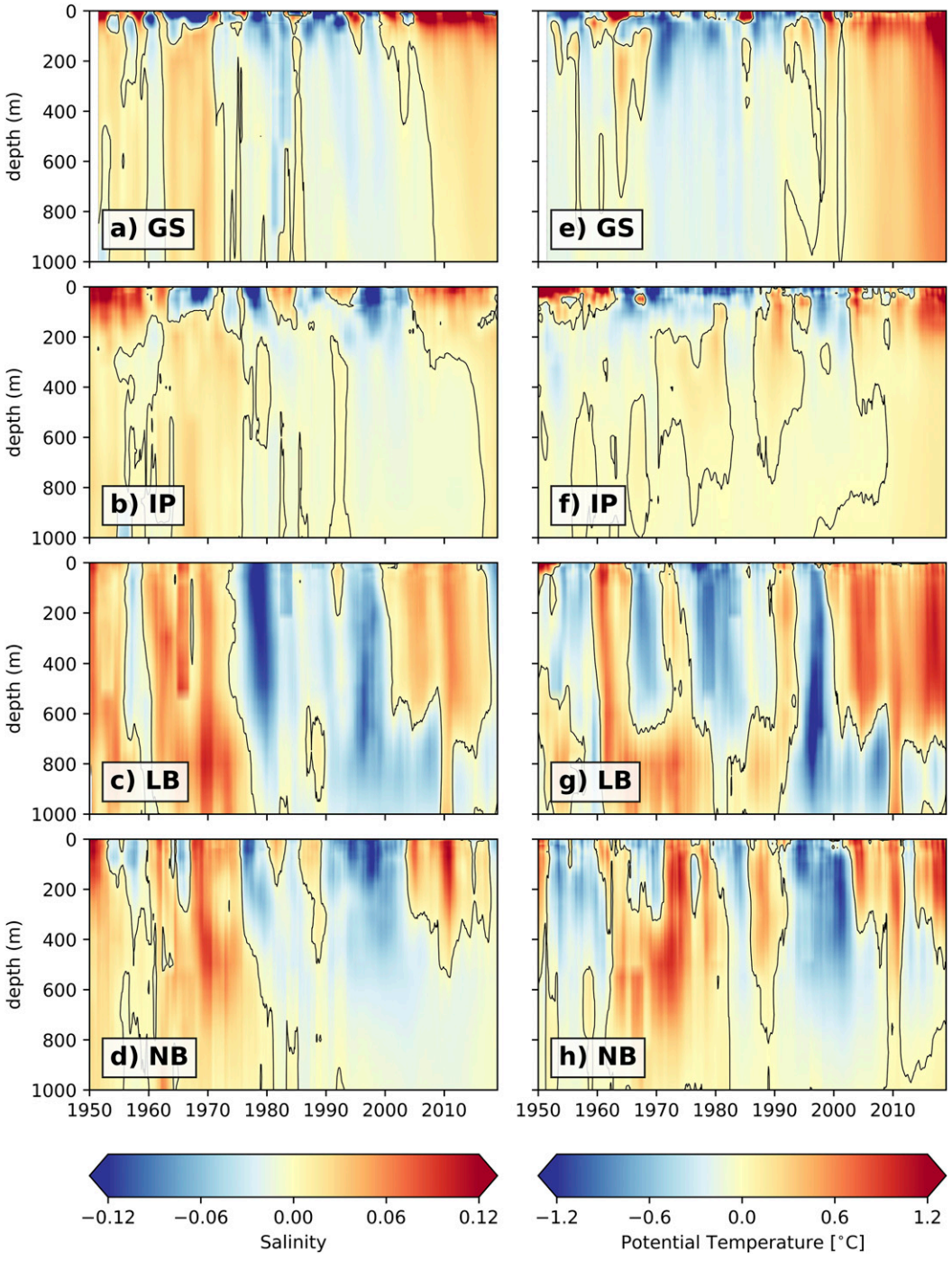

FIG. 3. Time series of (a)–(d) salinity and (e)–(h) potential temperature anomalies derived from the EN4 quality-controlled profiles averaged in the deep basins [Greenland Sea (GS), Lofoten Basin (LB), Norwegian Basin (NB), and Icelandic Plateau (IP)] of the Nordic seas for 1950–2018. Anomalies are relative to the 1950–2018 mean and are based on interpolated monthly means. Data are smoothed with a 25-month centered moving average. The black line indicates the zero contour.

The relationship between SAF position and the large-scale atmospheric forcing may be seen by examining two years of opposing SPG circulation extremes, as indicated by the SSH anomalies: 2010 (weak SPG) and 2015 (strong SPG), Figs. 6e and 6f. The SAF was displaced northwestward (southeastward) of its mean position in 2010 (2015) (Figs. 6a–d).

When the SPG was weak (2010), compared to 2015 the upper water column of the intergyre region (straddling the SPG

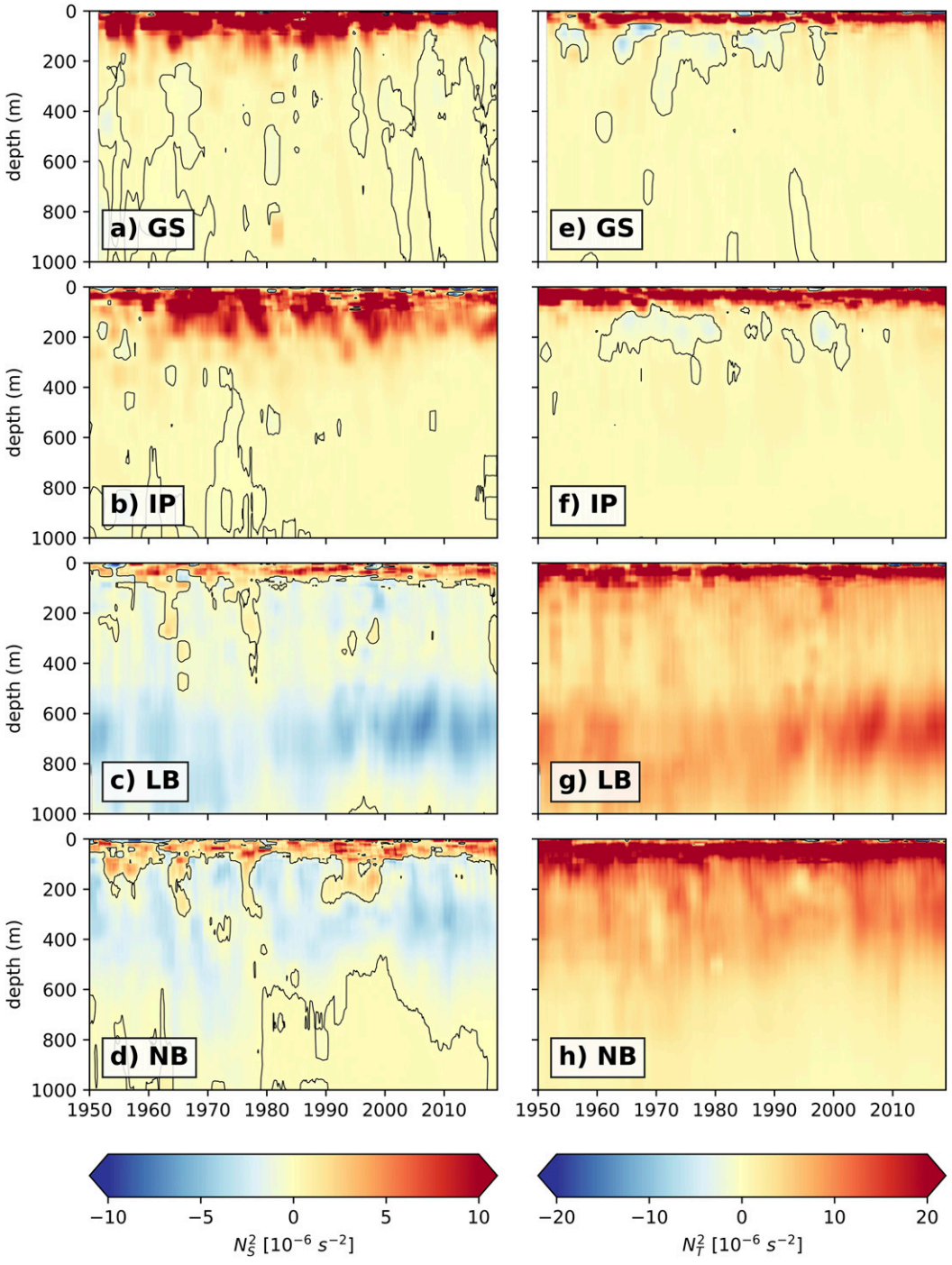

FIG. 4. Time series of (a)–(d) N_S^2 and (e)–(h) N_T^2 derived from the EN4 quality-controlled profiles averaged in the deep basins [Greenland Sea (GS), Lofoten Basin (LB), Norwegian Basin (NB), and Icelandic Plateau (IP)] of the Nordic seas for 1950–2018. Data are interpolated monthly means, smoothed with a 25-month centered moving average. The black line indicates the zero contour.

and STG) near ~20°–30°W was characterized by a greater contribution of temperature gradients to the stratification (and a destabilizing contribution from salinity gradients, $N_S^2 < 0$; Figs. 6a–d). The distinction between the two years is clear throughout the upper water column (Fig. 7). The entire upper water column was fresher farther to the south in 2015 compared to 2010 (Figs. 7a–c), and was more strongly stratified by salinity (Figs. 7d–f). This is evidence that these changing water-mass properties relate

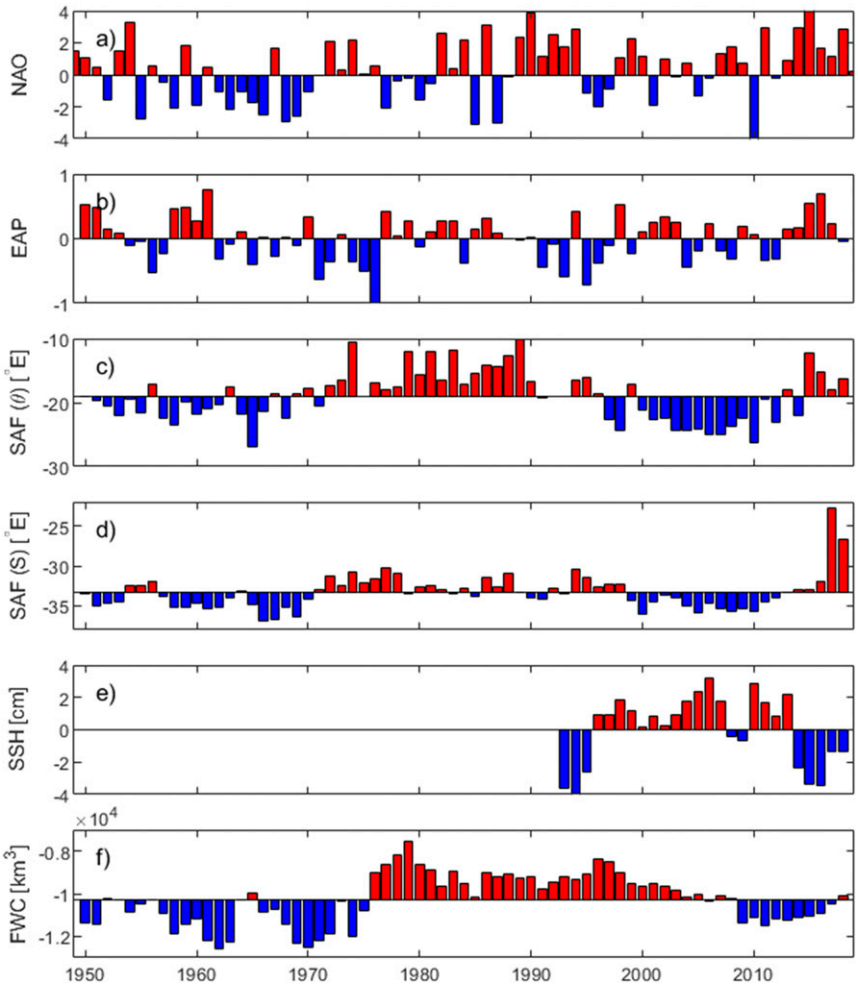

FIG. 5. (a) Annual mean NAO index. (b) Annual mean EAP index (detrended). (c) Longitude of the easternmost extent of the SAF at 60°N from the EN4 annual mean objective analysis during 1950–2018 (defined as the longitude of the 10°C isotherm at 10 m). Note that for certain latitudes and years, a particular isosurface of a water property may not intersect a depth surface within the defined study area and a value for the SAF index is not reported. (d) As in (c), but SAF is defined by the longitude of the 35.0 isohaline at 250 m, based on the criteria of Sarafanov et al. (2008). (e) Annual mean SSH anomaly relative to the 1992–2018 mean with linear trend removed over the SPG (approximately bounded by 50°–65°N, 60°–25°W) from the SSALTO/DUACS multisatellite altimetry product. (f) Annual mean FWC of the Nordic seas between 2000 m and the surface relative to 34.8 (note negative values relative to this reference salinity), calculated from the EN4 objective analysis. Red (blue) bars indicate years for which the FWC is greater than (less than) the time mean.

directly to a shift in the SAF. In 2010 the water-mass distribution suggests northward penetration of subtropical water into the Nordic seas, while its penetration was limited in 2015. The years 2010 and 2015 were characterized by strong, opposing anomalies of the NAO (Fig. 5a) and wind stress curl (Figs. 6g,h).

The case study described above is consistent with relationships over the full record analyzed. First, variations of the zonal SAF position (inferred from both isohaline and isotherm tracking) correlate with the SSH-based index of the gyre circulation for 1992–2018 (Figs. 5c–e; $r = -0.71$, $p < 0.01$ for the isotherm-based SAF index), confirming that a strong SPG coincides with an eastward displacement of the SAF, and vice versa. Second, the SAF position and SPG strength are closely linked to the Nordic seas FWC on interannual to decadal time scales over 1950–2018 (Figs. 5c,f). For instance, the decadal salinification trend of the Nordic seas beginning in the late 1990s was accompanied by a westward shift of the SAF. The FWC of the Nordic seas lags the isotherm-based SAF position by 5 years ($r = 0.61$, $p < 0.01$), with a similar relationship to the isohaline-based SAF position (Figs. 5c,d,f). This is consistent with the composition of the Atlantic inflow (which influences Nordic seas FWC) being regulated by SAF displacements. We further note

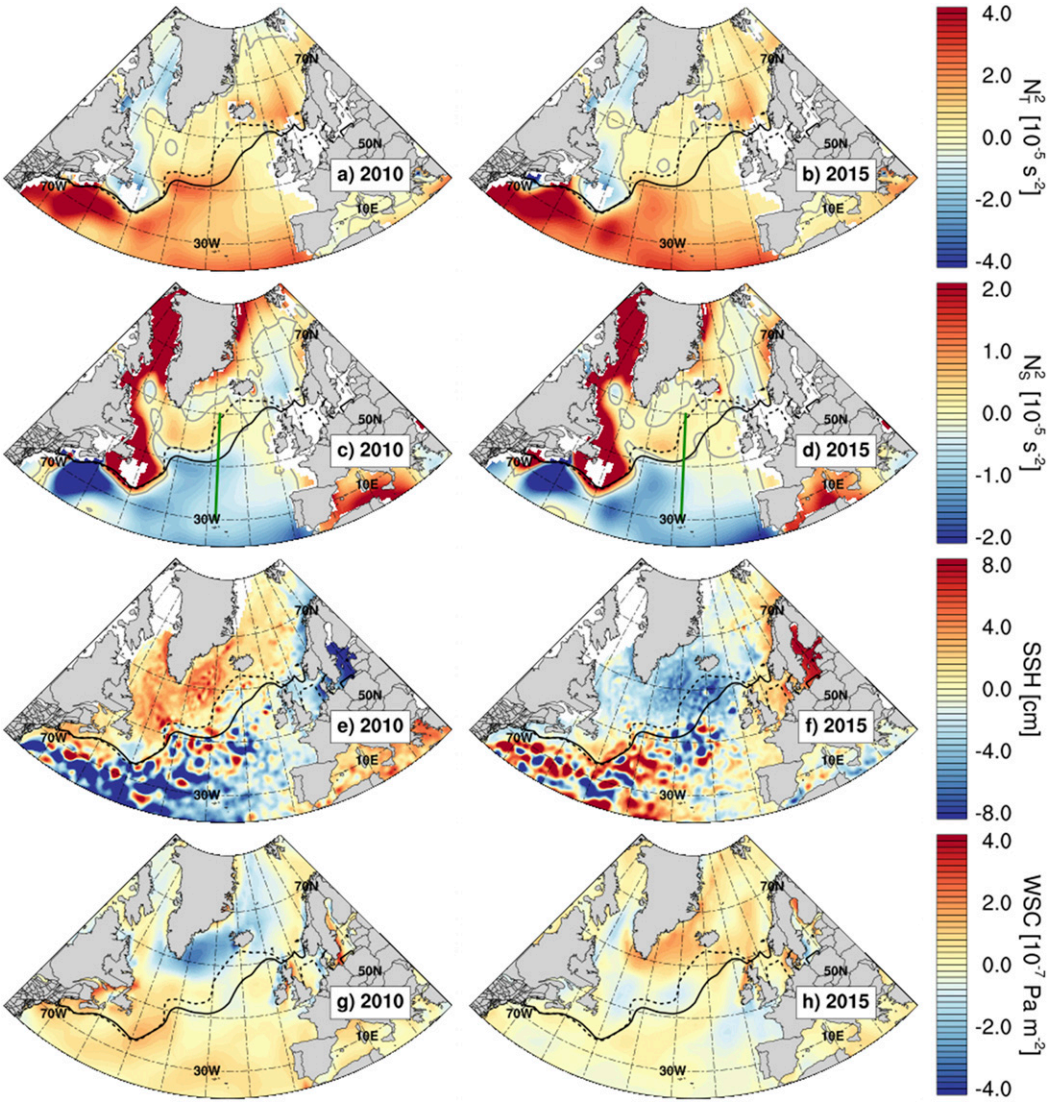

FIG. 6. (a),(b) Annual mean N_T^2 at ~210 m from the EN4 objective analysis for 2010 and 2015, respectively. The gray line indicates the zero contour. Black lines indicate the 10° isotherm at 10 m in 2010 (dashed contour) and 2015 (solid contour). (c),(d) As in (a) and (b), but for N_S^2. The green line indicates the location of the meridional transect in Fig. 7. (e),(f) Annual mean SSH anomaly relative to the 1993–2018 period for 2010 and 2015, respectively, from the SSALTO/DUACS gridded multisatellite altimetry product. To remove the sea level rise signal, the linear trend is removed from each grid point. (g),(h) Annual mean wind stress curl (WSC) anomaly relative to the 1990–2018 period for 2010 and 2015, respectively, from the NCEP/NCAR Reanalysis I.

that NAO-linked forcing influences the SAF position on decadal time scales ($r = 0.64$, $p < 0.05$ for the correlation of the isohaline-based SAF index and the NAO considering 5-yr mean time series with the NAO lagging by 2 years; the relationship to the isotherm-based index is less robust). See also Lozier and Stewart (2008). We corroborate these general relationships via an examination in the next section of a recent Nordic seas freshening related to an SAF displacement.

d. Freshening of the Nordic seas linked to SPG dynamics

To clarify the relationship between SAF displacements and the Nordic seas hydrography, it is instructive to examine a recent freshening event linking the SPG to the Nordic seas. In 2015, a prominent freshwater anomaly was present in the intergyre region (~30°W, 50°N; Figs. 7a–c and 8c). From the intergyre region, the fresh anomaly was apparently advected to reach the Nordic seas' Atlantic Domain by 2018 via the Atlantic inflow (Fig. 8f). This freshening event marked the end of the anomalously warm and saline period in the Nordic seas (Fig. 5f). As noted previously, the Beaufort Gyre circulation has been unfavorable for freshwater release during 1997–2018 (Proshutinsky et al. 2019a,b), and observations do not indicate a freshwater pulse at Fram Strait or Davis Strait in recent years that could account for the anomaly.

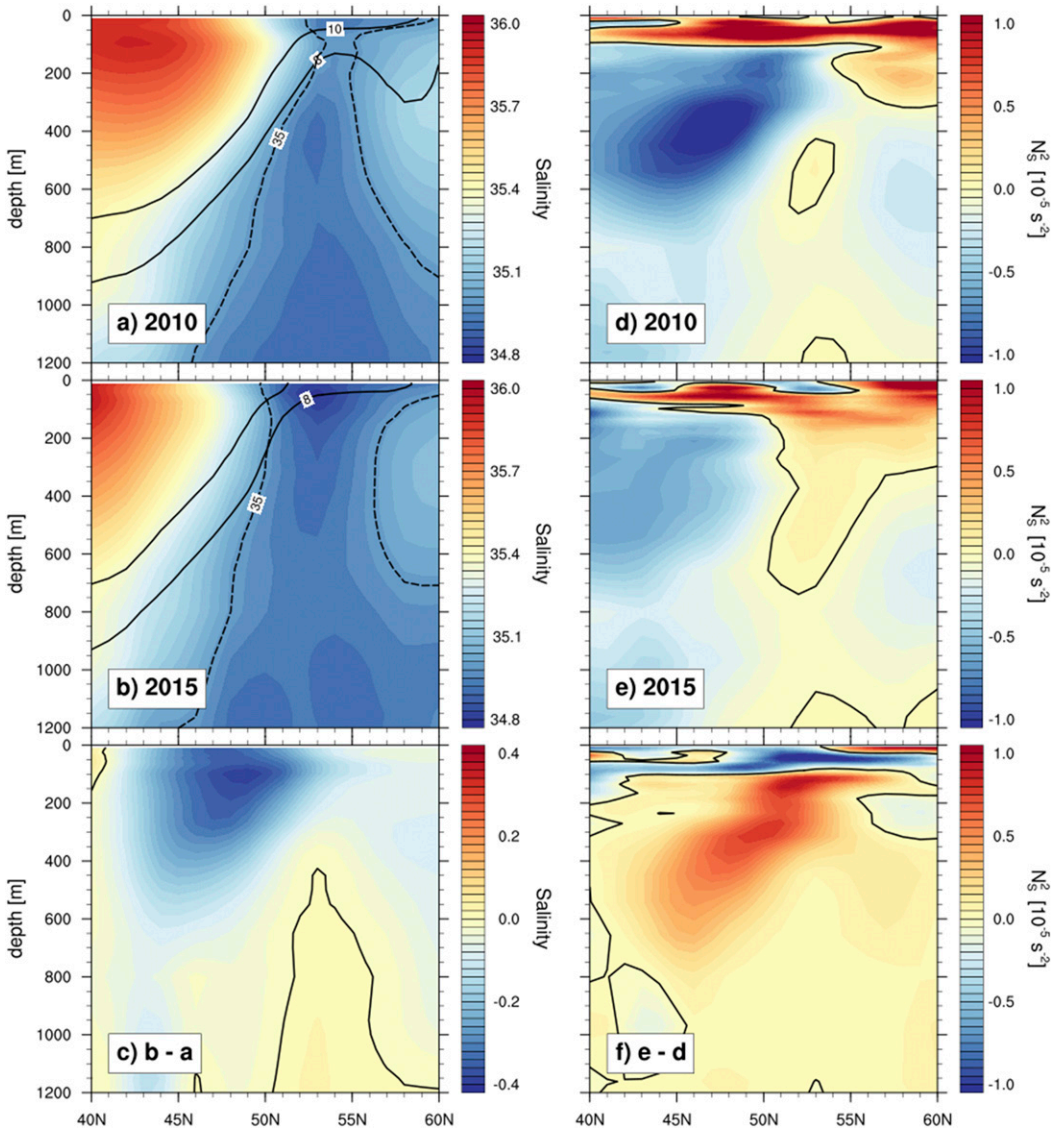

FIG. 7. (a),(b) Meridional transect of salinity at 28°W from the EN4 objective analysis for years 2010 and 2015, respectively. Location of the transect is indicated in Figs. 6c and 6d (solid green line). Solid black contours indicate the 10° and 8°C isotherms of potential temperature; the dashed black contour indicates the 35.0 isohaline. (c) Difference between (b) and (a). The black line indicates the zero contour. (d),(e) As in (a) and (b), but for N_S^2. The black line indicates the zero contour. (f) Difference between (e) and (d). The black line indicates the zero contour.

Holliday et al. (2020) describe this recent freshening as being related to NAO- and EAP-linked wind stress curl anomalies that diverted the Labrador Current offshore from the northwest North Atlantic shelf, causing a freshwater anomaly to develop there in 2012. They put forward that the eastward advection of the Labrador Current water during 2012–16 was the dominant contributor to the freshening of the eastern SPG; the result was a dipole in upper-ocean salinity between the northwest North Atlantic shelf (anomalously saline) and the eastern subpolar North Atlantic (anomalously fresh). The disappearance of the fresh anomaly in the central North Atlantic in 2013 (Fig. 2 of Holliday et al. 2020) would appear to be inconsistent, however, with the advection of the signal from the western basin. Although the analysis of Holliday et al. (2020) ends in 2016, the freshening signal was evident in the Atlantic Domain of the Nordic seas by 2017–18 (Figs. 8e,f).

It is possible that the development of this salinity dipole between the eastern and western basin (see, e.g., Fig. 8d) could be explained by wind-driven displacements of the SAF, without requiring a large-scale redistribution of the Labrador Current inflow. The 2014–16 period was characterized by strong positive NAO forcing (as well as EAP; see Figs. 5a,b), which relates to the observed eastward shift of the SAF (Figs. 5c,d) during this period. The eastward shift of the SAF

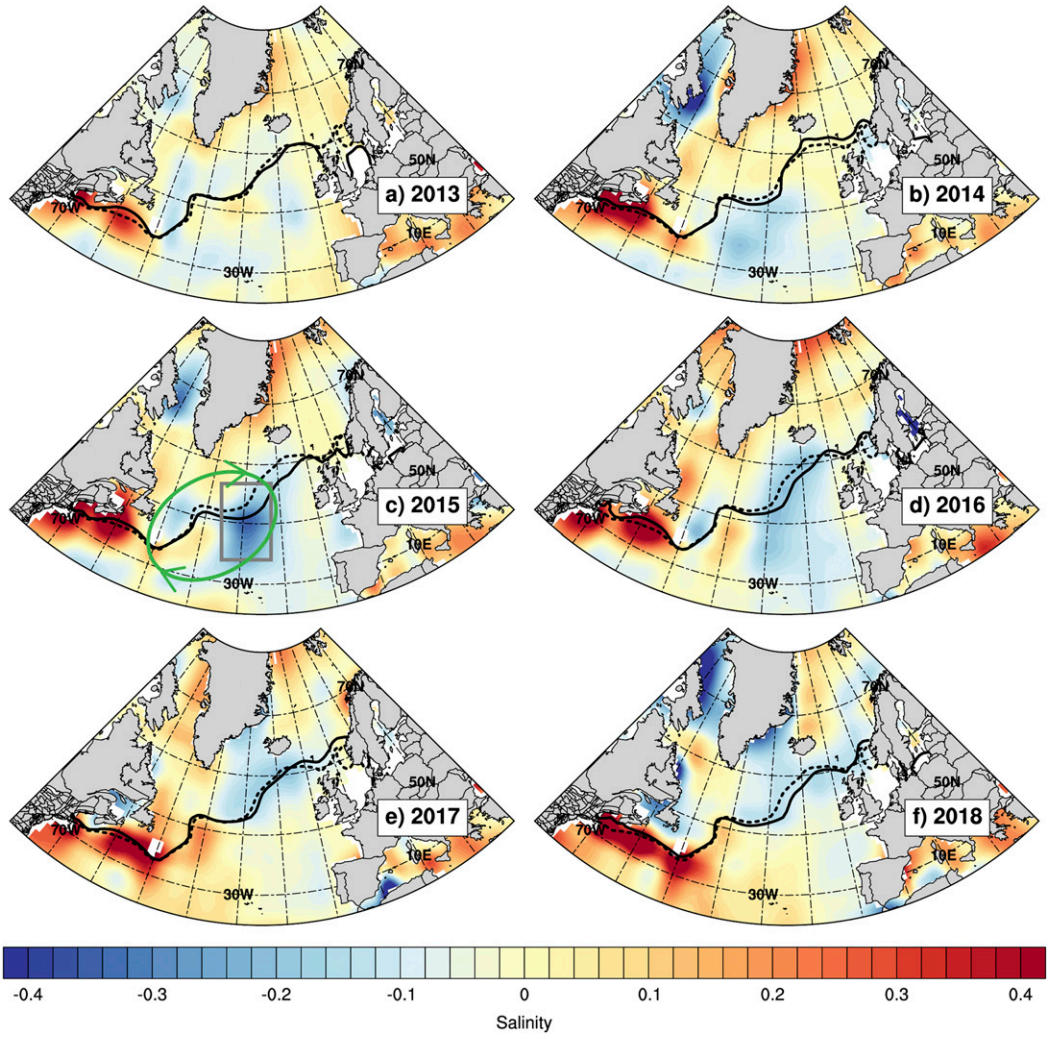

FIG. 8. Annual mean salinity anomaly at 100 m relative to the 1990–2018 period from the EN4 objective analysis for years (a)–(f) 2013–18. Black lines indicate the 10° isotherm at 10 m in the annual mean (solid contour) and during 1990–2018 (dashed contour). The green arrow and gray box in (c) represent the intergyre gyre circulation anomaly and the location of the fresh anomaly in the eastern basin, respectively.

gives rise to an anomalous intrusion of fresher SPG-type water masses into the northeastern North Atlantic Ocean. Similarly, positive NAO forcing has been shown to correspond to a northward shift of the SAF in the Newfoundland Basin and a positive salinity anomaly associated with the intrusion of STG water (see Núñez-Riboni et al. 2012), which could explain the salinity dipole pattern.

The relationship between the NAO, gyre circulation, and SAF displacements has been explained via an analytical model in which wind stress curl anomalies associated with a positive NAO phase induce a barotropic anticyclonic ocean circulation anomaly between the SPG and STG, i.e., an *intergyre gyre* (Marshall et al. 2001). This response has been demonstrated in model studies, and it has been shown that the northeastward flowing branch of the anticyclonic intergyre gyre advects relatively cold freshwater in the SPG, leading to a southeastward displacement of the SAF in the eastern North Atlantic Ocean (see Eden and Willebrand 2001). Herbaut and Houssais (2009) perform OGCM experiments to show that sustained atmospheric forcing similar to an NAO-positive state leads to a large-scale freshening of the eastern North Atlantic SPG and salinification near the northwest North Atlantic shelf after ~5 years. Using sensitivity experiments, they attributed these changes to anomalous wind-driven circulation rather than anomalous buoyancy fluxes or Arctic Ocean freshwater exports via the Labrador Current.

Whatever the precise mechanism responsible for the recent freshening in the Nordic seas, it is clear that North Atlantic Ocean circulation changes associated with SAF shifts played a major role. The freshening of the northeast North Atlantic Ocean in 2015 was characterized by a profound strengthening of the SPG (Figs. 5e and 6f) and an eastward displacement of SPG-type water masses in the eastern basin (Figs. 6b,d and 7b,c,e,f). The eastward shift of the SAF resulted in the

advection of a fresh anomaly to the Nordic seas via the Atlantic inflow in 2016–18 (Figs. 8c–f). The recent Nordic seas freshening is consistent with the concept that the water mass pathway from the Arctic Ocean to the Nordic seas is modulated by the SAF position.

4. Summary and conclusions

In one view, the Nordic seas and Beaufort Gyre are coupled directly via oceanic (and atmospheric) exchanges (e.g., Proshutinsky et al. 2015). In another view, the Atlantic inflow primarily determines the properties of the Nordic seas, leaving a minor role for Arctic Ocean exports (Glessmer et al. 2014). In this study, we have examined time series (1950–2018) of hydrography, FWC, atmospheric forcing, and SPG configurations that suggest a synthesized view: while Arctic fluxes, whether less fresh or more fresh, may ultimately influence the hydrography of the Nordic seas, they do so predominantly by indirect means, via the SPG, and therefore their influence relies upon how much the SPG influences the Nordic seas.

We have examined case studies of two years with anomalous NAO conditions (2010 and 2015) to show how the SPG influence on the Nordic seas is determined by North Atlantic Ocean dynamics (such as the wind-driven NAO-linked barotropic circulation) that control the position of the SAF, and therefore the relative contributions STG and SPG water masses. This is supported by our examination of the relative contributions of vertical temperature and salinity gradients (N_T^2, N_S^2) to the stratification.

In the Nordic seas, cool and fresh conditions through the entire upper water column have alternated with warm and saline conditions on decadal time scales. Recently, the FWC of the Nordic seas declined during 1997–2015, a trend that abruptly reversed after ~2016. Arctic Ocean freshwater exports alone cannot explain these phenomena (setting aside uncertainties in the data). Rather, recent changes in the Nordic seas FWC are likely related to SAF displacements, which modify the contribution of SPG and STG parent waters to the Atlantic inflow.

The increase in the Nordic seas FWC after ~2016 is linked to the advection by the Atlantic inflow of a fresh anomaly that formed in the eastern SPG in the mid-2010s. Holliday et al. (2020) have primarily attributed this SPG fresh anomaly to wind-induced ocean circulation changes, leading to a redistribution of the Labrador Current inflow and a salinity dipole (i.e., freshening of the eastern SPG and salinification in the northwest North Atlantic shelf). In this view, the displacement of the SAF and enhanced Arctic Ocean exports are second-order factors. We propose the alternative hypothesis that the salinity dipole pattern could be explained by the NAO-linked intergyre gyre anomaly, inducing opposing SAF displacements in the eastern and western basin. In this case, the large-scale redistribution of the Labrador Current inflow would not be necessary to explain this spatial pattern. Our SSH-based SPG index and SAF indices corroborate an intensification of the SPG and an eastward shift of the SAF during this period (Figs. 5c–e). While the intergyre gyre has been well characterized in OGCM modeling studies with idealized forcing, further research is needed to identify its signature in observational data. In either case, this event demonstrates that the advection of GSA-like anomalies (whether formed remotely in the Arctic or locally) from the SPG to the Nordic seas via the Atlantic inflow is related to the eastward displacement of the SAF.

Our results suggest that the NAO phase may play a dual role in the transport of Arctic Ocean freshwater anomalies to the Nordic seas. NAO-positive conditions have been associated with wind-driven Arctic Ocean circulation changes that lead to enhanced freshwater exports to the North Atlantic Ocean (Karcher et al. 2005; Peterson et al. 2006); these conditions may also enhance the penetration of Arctic/SPG water masses to the Atlantic inflow to the Nordic seas.

Lauvset et al. (2018) have found that the warming and salinification of the Greenland Sea since the early 2000s have resulted in increased mixed layer depths and oxygen concentrations (indicative of recent ventilation). While recent research has anticipated an Atlantification of the Nordic seas' Arctic domain (i.e., a shift to warmer and saltier conditions) as a consequence of climate change, our research suggests that such shifts may also result from SPG circulation variability on decadal time scales. Through this mechanism, SPG dynamics could have potentially important implications for the thermohaline circulation.

Acknowledgments. J.S. Kenigson acknowledges the support of the Yale Institute for Biospheric Studies (YIBS) Donnelley Fellowship. M.-L. Timmermans acknowledges funding provided by the National Science Foundation Office of Polar Programs under Award 1950077.

Data availability statement. The EN4.2.1 data (Good et al. 2013) are available from the Met Office Hadley Centre (https://www.metoffice.gov.uk/hadobs/en4/). The XBT and MBT data are bias-corrected using the procedures of Gouretski and Reseghetti (2010). This study has been conducted using E.U. Copernicus Marine Service Information (the SSALTO/DUACS absolute dynamic topography product; Taburet et al. 2019). The annual mean station-based NAO index (Hurrell 1995) is available from the NCAR Climate Analysis Section (https://climatedataguide.ucar.edu/climate-data/hurrell-north-atlantic-oscillation-nao-index-station-based). The monthly mean EAP index is available from the NOAA National Weather Service Climate Prediction Center (https://www.cpc.ncep.noaa.gov/data/teledoc/ea.shtml). The NCEP/NCAR Reanalysis I wind stress curl data (Kalnay et al. 1996) are available from the KNMI Climate Explorer database (https://climexp.knmi.nl).

REFERENCES

Aagaard, K., and E. C. Carmack, 1989: The role of sea ice and other fresh water in the Arctic circulation. *J. Geophys. Res.*, **94**, 14 485–14 498, https://doi.org/10.1029/JC094iC10p14485.

Amante, C., and B. Eakins, 2009: ETOPO1 1 arc-minute global relief model: Procedures, data sources and analysis. NOAA Tech. Memo. NESDIS NGDC-24, 25 pp., https://www.ngdc.noaa.gov/mgg/global/relief/ETOPO1/docs/ETOPO1.pdf.

Årthun, M., T. Eldevik, L. Smedsrud, Ø. Skagseth, and R. Ingvaldsen, 2012: Quantifying the influence of Atlantic heat on Barents Sea

ice variability and retreat. *J. Climate*, **25**, 4736–4743, https://doi.org/10.1175/JCLI-D-11-00466.1.

Barnston, A. G., and R. E. Livezey, 1987: Classification, seasonality and persistence of low-frequency atmospheric circulation patterns. *Mon. Wea. Rev.*, **115**, 1083–1126, https://doi.org/10.1175/1520-0493(1987)115<1083:CSAPOL>2.0.CO;2.

Belkin, I. M., 2004: Propagation of the ''Great Salinity Anomaly'' of the 1990s around the northern North Atlantic. *Geophys. Res. Lett.*, **31**, L08306, https://doi.org/10.1029/2003GL019334.

——, and S. Levitus, 1996: Temporal variability of the subarctic front near the Charlie-Gibbs fracture zone. *J. Geophys. Res.*, **101**, 28 317–28 324, https://doi.org/10.1029/96JC02794.

——, ——, J. Antonov, and S.-A. Malmberg, 1998: ''Great Salinity Anomalies'' in the North Atlantic. *Prog. Oceanogr.*, **41**, 1–68, https://doi.org/10.1016/S0079-6611(98)00015-9.

Bersch, M., I. Yashayaev, and K. P. Koltermann, 2007: Recent changes of the thermohaline circulation in the subpolar North Atlantic. *Ocean Dyn.*, **57**, 223–235, https://doi.org/10.1007/s10236-007-0104-7.

Berx, B., and M. Payne, 2017: The Sub-Polar Gyre Index-A community data set for application in fisheries and environment research. *Earth Syst. Sci. Data*, **9**, 259–266, https://doi.org/10.5194/essd-9-259-2017.

Carmack, E. C., 2007: The alpha/beta ocean distinction: A perspective on freshwater fluxes, convection, nutrients and productivity in high-latitude seas. *Deep-Sea Res. II*, **54**, 2578–2598, https://doi.org/10.1016/j.dsr2.2007.08.018.

Chafik, L., and T. Rossby, 2019: Volume, heat, and freshwater divergences in the subpolar North Atlantic suggest the Nordic Seas as key to the state of the meridional overturning circulation. *Geophys. Res. Lett.*, **46**, 4799–4808, https://doi.org/10.1029/2019GL082110.

Curry, B., C. Lee, B. Petrie, R. Moritz, and R. Kwok, 2014: Multiyear volume, liquid freshwater, and sea ice transports through Davis Strait, 2004–10. *J. Phys. Oceanogr.*, **44**, 1244–1266, https://doi.org/10.1175/JPO-D-13-0177.1.

Curry, R., and C. Mauritzen, 2005: Dilution of the northern North Atlantic Ocean in recent decades. *Science*, **308**, 1772–1774, https://doi.org/10.1126/science.1109477.

de Steur, L., E. Hansen, R. Gerdes, M. Karcher, E. Fahrbach, and J. Holfort, 2009: Freshwater fluxes in the east Greenland current: A decade of observations. *Geophys. Res. Lett.*, **36**, L23611, https://doi.org/10.1029/2009GL041278.

——, R. S. Pickart, A. Macrander, K. Våge, B. Harden, S. Jónsson, S. Østerhus, and H. Valdimarsson, 2017: Liquid freshwater transport estimates from the East Greenland Current based on continuous measurements north of Denmark Strait. *J. Geophys. Res. Oceans*, **122**, 93–109, https://doi.org/10.1002/2016JC012106.

——, C. Peralta-Ferriz, and O. Pavlova, 2018: Freshwater export in the East Greenland current freshens the North Atlantic. *Geophys. Res. Lett.*, **45**, 13 359–13 366, https://doi.org/10.1029/2018GL080207.

Dickson, R. R., J. Meincke, S.-A. Malmberg, and A. J. Lee, 1988: The ''Great Salinity Anomaly'' in the northern North Atlantic 1968–1982. *Prog. Oceanogr.*, **20**, 103–151, https://doi.org/10.1016/0079-6611(88)90049-3.

Dukhovskoy, D. S., M. A. Johnson, and A. Proshutinsky, 2004: Arctic decadal variability: An auto-oscillatory system of heat and fresh water exchange. *Geophys. Res. Lett.*, **31**, L03302, https://doi.org/10.1029/2003GL019023.

——, ——, and ——, 2006a: Arctic decadal variability from an idealized atmosphere-ice-ocean model: 1. Model description, calibration, and validation. *J. Geophys. Res.*, **111**, C06028, https://doi.org/10.1029/2004JC002821.

——, ——, and ——, 2006b: Arctic decadal variability from an idealized atmosphere-ice-ocean model: 2. Simulation of decadal oscillations. *J. Geophys. Res.*, **111**, C06029, https://doi.org/10.1029/2004JC002820.

Eden, C., and J. Willebrand, 2001: Mechanism of interannual to decadal variability of the North Atlantic circulation. *J. Climate*, **14**, 2266–2280, https://doi.org/10.1175/1520-0442(2001)014<2266:MOITDV>2.0.CO;2.

Florindo-López, C., S. Bacon, Y. Aksenov, L. Chafik, E. Colbourne, and N. P. Holliday, 2020: Arctic Ocean and Hudson Bay freshwater exports: New estimates from seven decades of hydrographic surveys on the Labrador Shelf. *J. Climate*, **33**, 8849–8868, https://doi.org/10.1175/JCLI-D-19-0083.1.

Foukal, N. P., and M. S. Lozier, 2017: Assessing variability in the size and strength of the North Atlantic subpolar gyre. *J. Geophys. Res. Oceans*, **122**, 6295–6308, https://doi.org/10.1002/2017JC012798.

Giles, K. A., S. W. Laxon, A. L. Ridout, D. J. Wingham, and S. Bacon, 2012: Western Arctic Ocean freshwater storage increased by wind-driven spin-up of the Beaufort Gyre. *Nat. Geosci.*, **5**, 194–197, https://doi.org/10.1038/ngeo1379.

Glessmer, M. S., T. Eldevik, K. Våge, J. E. Ø. Nilsen, and E. Behrens, 2014: Atlantic origin of observed and modelled freshwater anomalies in the Nordic Seas. *Nat. Geosci.*, **7**, 801–805, https://doi.org/10.1038/ngeo2259.

Good, S. A., M. J. Martin, and N. A. Rayner, 2013: EN4: Quality controlled ocean temperature and salinity profiles and monthly objective analyses with uncertainty estimates. *J. Geophys. Res. Oceans*, **118**, 6704–6716, https://doi.org/10.1002/2013JC009067.

Gouretski, V., and F. Reseghetti, 2010: On depth and temperature biases in bathythermograph data: Development of a new correction scheme based on analysis of a global ocean database. *Deep-Sea Res. I*, **57**, 812–833, https://doi.org/10.1016/j.dsr.2010.03.011.

Grist, J. P., S. A. Josey, Z. L. Jacobs, R. Marsh, B. Sinha, and E. Van Sebille, 2016: Extreme air–sea interaction over the North Atlantic subpolar gyre during the winter of 2013–2014 and its sub-surface legacy. *Climate Dyn.*, **46**, 4027–4045, https://doi.org/10.1007/s00382-015-2819-3.

Haine, T. W., and Coauthors, 2015: Arctic freshwater export: Status, mechanisms, and prospects. *Global Planet. Change*, **125**, 13–35, https://doi.org/10.1016/j.gloplacha.2014.11.013.

Häkkinen, S., and P. B. Rhines, 2004: Decline of subpolar North Atlantic circulation during the 1990s. *Science*, **304**, 555–559, https://doi.org/10.1126/science.1094917.

——, ——, and D. L. Worthen, 2011: Warm and saline events embedded in the meridional circulation of the northern North Atlantic. *J. Geophys. Res.*, **116**, C03006, https://doi.org/10.1029/2010JC006275.

Hansen, B., and S. Østerhus, 2000: North Atlantic-Nordic Seas exchanges. *Prog. Oceanogr.*, **45**, 109–208, https://doi.org/10.1016/S0079-6611(99)00052-X.

Hátún, H., and L. Chafik, 2018: On the recent ambiguity of the North Atlantic subpolar gyre index. *J. Geophys. Res. Oceans*, **123**, 5072–5076, https://doi.org/10.1029/2018JC014101.

——, A. B. Sandø, H. Drange, B. Hansen, and H. Valdimarsson, 2005: Influence of the Atlantic subpolar gyre on the thermohaline circulation. *Science*, **309**, 1841–1844, https://doi.org/10.1126/science.1114777.

Herbaut, C., and M.-N. Houssais, 2009: Response of the eastern North Atlantic subpolar gyre to the North Atlantic oscillation.

Geophys. Res. Lett., **36**, L17607, https://doi.org/10.1029/2009GL039090.

Holliday, N. P., and Coauthors, 2020: Ocean circulation causes the largest freshening event for 120 years in eastern subpolar North Atlantic. *Nat. Commun.*, **11**, 585, https://doi.org/10.1038/s41467-020-14474-y.

Hurrell, J. W., 1995: Decadal trends in the North Atlantic Oscillation: Regional temperatures and precipitation. *Science*, **269**, 676–679, https://doi.org/10.1126/science.269.5224.676.

Josey, S. A., J. J.-M. Hirschi, B. Sinha, A. Duchez, J. P. Grist, and R. Marsh, 2018: The recent Atlantic cold anomaly: Causes, consequences, and related phenomena. *Annu. Rev. Mar. Sci.*, **10**, 475–501, https://doi.org/10.1146/annurev-marine-121916-063102.

Kalnay, E., and Coauthors, 1996: The NCEP/NCAR 40-Year Reanalysis Project. *Bull. Amer. Meteor. Soc.*, **77**, 437–472, https://doi.org/10.1175/1520-0477(1996)077<0437:TNYRP>2.0.CO;2.

Karcher, M., R. Gerdes, F. Kauker, C. Köberle, and I. Yashayaev, 2005: Arctic Ocean change heralds North Atlantic freshening. *Geophys. Res. Lett.*, **32**, L21606, https://doi.org/10.1029/2005GL023861.

Latarius, K., and D. Quadfasel, 2016: Water mass transformation in the deep basins of the Nordic Seas: Analyses of heat and freshwater budgets. *Deep-Sea Res. I*, **114**, 23–42, https://doi.org/10.1016/j.dsr.2016.04.012.

Lauvset, S. K., A. Brakstad, K. Våge, A. Olsen, E. Jeansson, and K. A. Mork, 2018: Continued warming, salinification and oxygenation of the Greenland Sea gyre. *Tellus*, **70A**, 1–9, https://doi.org/10.1080/16000870.2018.1476434.

Lozier, M. S., and N. M. Stewart, 2008: On the temporally varying northward penetration of Mediterranean Overflow Water and eastward penetration of Labrador Sea Water. *J. Phys. Oceanogr.*, **38**, 2097–2103, https://doi.org/10.1175/2008JPO3908.1.

——, and Coauthors, 2019: A sea change in our view of overturning in the subpolar North Atlantic. *Science*, **363**, 516–521, https://doi.org/10.1126/science.aau6592.

Marshall, J., H. Johnson, and J. Goodman, 2001: A study of the interaction of the North Atlantic Oscillation with ocean circulation. *J. Climate*, **14**, 1399–1421, https://doi.org/10.1175/1520-0442(2001)014<1399:ASOTIO>2.0.CO;2.

McDougall, T. J., and P. M. Barker, 2011: Getting started with TEOS-10 and the Gibbs Seawater (GSW) oceanographic toolbox. SCOR/IAPSO WG 127, 28 pp., http://www.teos-10.org/pubs/Getting_Started.pdf.

Mork, K. A., Ø. Skagseth, and H. Søiland, 2019: Recent warming and freshening of the Norwegian Sea observed by Argo data. *J. Climate*, **32**, 3695–3705, https://doi.org/10.1175/JCLI-D-18-0591.1.

Nilsen, J. E. Ø., and E. Falck, 2006: Variations of mixed layer properties in the Norwegian Sea for the period 1948–1999. *Prog. Oceanogr.*, **70**, 58–90, https://doi.org/10.1016/j.pocean.2006.03.014.

Núñez-Riboni, I., M. Bersch, H. Haak, and J. Jungclaus, 2012: A multi-decadal meridional displacement of the Subpolar Front in the Newfoundland Basin. *Ocean Sci.*, **8**, 91–102, https://doi.org/10.5194/os-8-91-2012.

Peterson, B. J., J. McClelland, R. Curry, R. M. Holmes, J. E. Walsh, and K. Aagaard, 2006: Trajectory shifts in the Arctic and subarctic freshwater cycle. *Science*, **313**, 1061–1066, https://doi.org/10.1126/science.1122593.

Proshutinsky, A., R. Bourke, and F. McLaughlin, 2002: The role of the Beaufort Gyre in Arctic climate variability: Seasonal to decadal climate scales. *Geophys. Res. Lett.*, **29**, 2100, https://doi.org/10.1029/2002GL015847.

——, and Coauthors, 2009: Beaufort Gyre freshwater reservoir: State and variability from observations. *J. Geophys. Res.*, **114**, C00A10, https://doi.org/10.1029/2008JC005104.

——, D. Dukhovskoy, M.-L. Timmermans, R. Krishfield, and J. L. Bamber, 2015: Arctic circulation regimes. *Philos. Trans. Roy. Soc.*, **373A**, 20140160, https://doi.org/10.1098/rsta.2014.0160.

——, R. Krishfield, and M.-L. Timmermans, 2019a: Preface to special issue Forum for Arctic Ocean Modeling and Observational Synthesis (FAMOS) 2: Beaufort Gyre phenomenon. *J. Geophys. Res. Oceans*, **125**, e2019JC015400, https://doi.org/10.1029/2019JC015400.

——, and Coauthors, 2019b: Analysis of the Beaufort Gyre freshwater content in 2003-2018. *J. Geophys. Res. Oceans*, **124**, 9658–9689, https://doi.org/10.1029/2019JC015281.

Reverdin, G., 2014: Oceanography: Freshened from the south. *Nat. Geosci.*, **7**, 783–784, https://doi.org/10.1038/ngeo2268.

Robson, J., P. Ortega, and R. Sutton, 2016: A reversal of climatic trends in the North Atlantic since 2005. *Nat. Geosci.*, **9**, 513–517, https://doi.org/10.1038/ngeo2727.

Roden, G. I., 1991: Subarctic-subtropical transition zone of the North Pacific: Large-scale aspects and mesoscale structure. Biology, oceanography, and fisheries of the North Pacific transition zone and subarctic frontal zone, J. A. Wetherall, Ed., NOAA Tech. Rep. NMFS 105, 1–38, https://repository.library.noaa.gov/view/noaa/6054.

Sarafanov, A., 2009: On the effect of the North Atlantic Oscillation on temperature and salinity of the subpolar North Atlantic intermediate and deep waters. *ICES J. Mar. Sci.*, **66**, 1448–1454, https://doi.org/10.1093/icesjms/fsp094.

——, A. Falina, A. Sokov, and A. Demidov, 2008: Intense warming and salinification of intermediate waters of southern origin in the eastern subpolar North Atlantic in the 1990s to mid-2000s. *J. Geophys. Res.*, **113**, C12022, https://doi.org/10.1029/2008JC004975.

Schauer, U., and M. Losch, 2019: "Freshwater" in the ocean is not a useful parameter in climate research. *J. Phys. Oceanogr.*, **49**, 2309–2321, https://doi.org/10.1175/JPO-D-19-0102.1.

Stewart, K. D., and T. W. Haine, 2016: Thermobaricity in the transition zones between alpha and beta oceans. *J. Phys. Oceanogr.*, **46**, 1805–1821, https://doi.org/10.1175/JPO-D-16-0017.1.

Taburet, G., A. Sanchez-Roman, M. Ballarotta, M.-I. Pujol, J.-F. Legeais, F. Fournier, Y. Faugere, and G. Dibarboure, 2019: DUACS DT2018: 25 years of reprocessed sea level altimetry products. *Ocean Sci.*, **15**, 1207–1224, https://doi.org/10.5194/os-15-1207-2019.

Visbeck, M., E. P. Chassignet, R. G. Curry, T. L. Delworth, R. R. Dickson, and G. Krahmann, 2003: The ocean's response to North Atlantic Oscillation variability. *The North Atlantic Oscillation: Climatic Significance and Environmental Impact, Geophys. Monogr.*, Vol. 134, Amer. Geophys. Union, 113–145.

Zhong, W., M. Steele, J. Zhang, and S. T. Cole, 2019: Circulation of Pacific winter water in the western Arctic Ocean. *J. Geophys. Res. Oceans*, **124**, 863–881, https://doi.org/10.1029/2018JC014604.